Natural Resources Research, Vol. 21, No. 2, June 2012 (© 2012)
DOI: 10.1007/s11053-012-9170-8

Geostatistical Modeling of Ore Grade Distribution from Geomorphic Characterization in a Laterite Nickel Deposit

Asran Ilyas[1] and Katsuaki Koike[2,3]

Received 11 July 2011; accepted 23 January 2012
Published online: 15 February 2012

Due to growing consumption of nickel (Ni) in a range of industries, the demand for Ni has increased rapidly around the world. This trend requires a more precise estimation of available Ni grade deposits and an identification of factors controlling the grade distribution. To achieve these requirements, this study applies geostatistical techniques to spatial modeling of the Ni grade in a laterite Ni deposit, with reference to geomorphic features such as slope gradient and the thickness of limonite and saprolite zones. The Sorowako area in Sulawesi Island, Indonesia, was chosen as a case study area because it has a representative laterite Ni deposit with large reserves. Chemical content data from drillhole cores at 294 points were used for the analysis. The slope gradient was found to have a remarkable correlation with the thickness of the limonite zone, but there was no correlation between the thickness of the limonite and the saprolite zones above the bedrock. One important feature was a general correlation between the thickness of the saprolite zone and the maximum Ni grade in this zone: the grade increases with the thickness of the zone. Co-kriging was adopted to incorporate this correlation into estimating the maximum Ni grade in the saprolite zone. As a result, the maximum Ni grade in the saprolite zone tends to be high mainly in areas of slight slope. The Ni accumulation at this topographic feature probably originates from deep weathering by groundwater infiltrating through well-developed rock fractures.

KEY WORDS: Co-kriging, slope gradient, limonite zone, saprolite zone, nickel grade, Sulawesi.

INTRODUCTION

Nickel (Ni) exists as a silvery-white lustrous metallic element that can withstand high temperatures. This characteristic is suitable for producing heat-resistant equipment such as aircraft engines. In addition, Ni has a stainless feature (USGS Mineral Commodity Summaries 2011), and has been widely used in alloys with other metals (Thompson 2000). Because of these two favorable metallic features, Ni has been used as a raw material for many kinds of industrial products, including steel, chemicals, electrical equipment, fabricated metals, household appliances, and machinery. Its major use is in stainless steel, which accounts for two-thirds of primary Ni production. The widespread consumption of Ni, along with the growth in new developments in the electronics and telecommunication industries, has seen the demand for Ni increase rapidly since 2000. This trend requires on-going exploration and exploitation of Ni deposits around the world, while ensuring Ni mining is sensitive to natural environments.

There are two types of Ni deposits with different mechanisms of formation. They are laterite and magmatic sulfide deposits. The principal ore minerals are nickeliferous limonite (Fe, Ni)O(OH) and garnierite (a hydrous nickel silicate) $(Ni, Mg)_3Si_2O_5(OH)_4$ of the laterite type and pentlandite $(Ni, Fe)_9S_8$ of the magmatic sulfide type. Laterite deposits are more

[1]Graduate School of Science and Technology, Kumamoto University, 2-39-1 Kurokami, Kumamoto 860-8555, Japan.
[2]Department of Urban Management, Graduate School of Engineering, Kyoto University, Katsura C1-2-215, Kyoto 615-8540, Japan.
[3]To whom correspondence should be addressed; e-mail: koike.katsuaki.5x@kyoto-u.ac.jp

important for land-based resources, because approximately 60% of Ni originates from laterite deposits out of a total of 130 million ton (Mt) (Gleeson et al. 2003). Laterite Ni deposits have been discovered dominantly in the tropical and subtropical belts (Gleeson et al. 2003; Thorne et al. 2009), and are generated by intense weathering of ultramafic igneous rocks, with the resulting secondary concentrations of Ni-bearing oxide and silicate minerals. This type of deposit is commonly derived from chemical weathering of olivine-rich cumulate rocks and their metamorphic derivatives, which have primary initial Ni contents of 0.2–0.4% (Brand et al. 1998).

Indonesia is one of the major countries rich in Ni resources and has world-famous large laterite deposits. In 2009, world Ni production had reached 1.43 Mt and approximately 13% of the production came from Indonesia. Indonesia is the second ranked country for Ni production (Price 2010; Sufriadin et al. 2010). Large laterite deposits are concentrated on Sulawesi Island, and Sorowako is a typical area containing a hydrous silicate deposit that has been developed since 1968 by a mining company, PT. INCO Indonesia (Fig. 1). It is well known that an accurate estimation of Ni reserves is difficult in laterite deposits because of the complexity of geological structure, local changes in degree of weathering even in the same lithology, strong heterogeneity of Ni grade distribution, differences in Ni concentration patterns such as vein or disseminated ore body, and the influence of many factors controlling the Ni grade.

Based on the above background information, this study is aimed at developing a method for precise spatial modeling of Ni grade in a laterite deposit. Our modeling process is implemented by identifying control factors on the grade distribution and applying geostatistical techniques. Precise Ni grade modeling can contribute to accurately assessing Ni reserves. The Sorowako area in Figure 1 is a representative laterite Ni deposit and considerable exploration data has been accumulated by PT. INCO Indonesia. Thus, the area was selected as a suitable test site for grade modeling. Among the many possible factors, a geomorphic factor is selected as the most dominant because it can

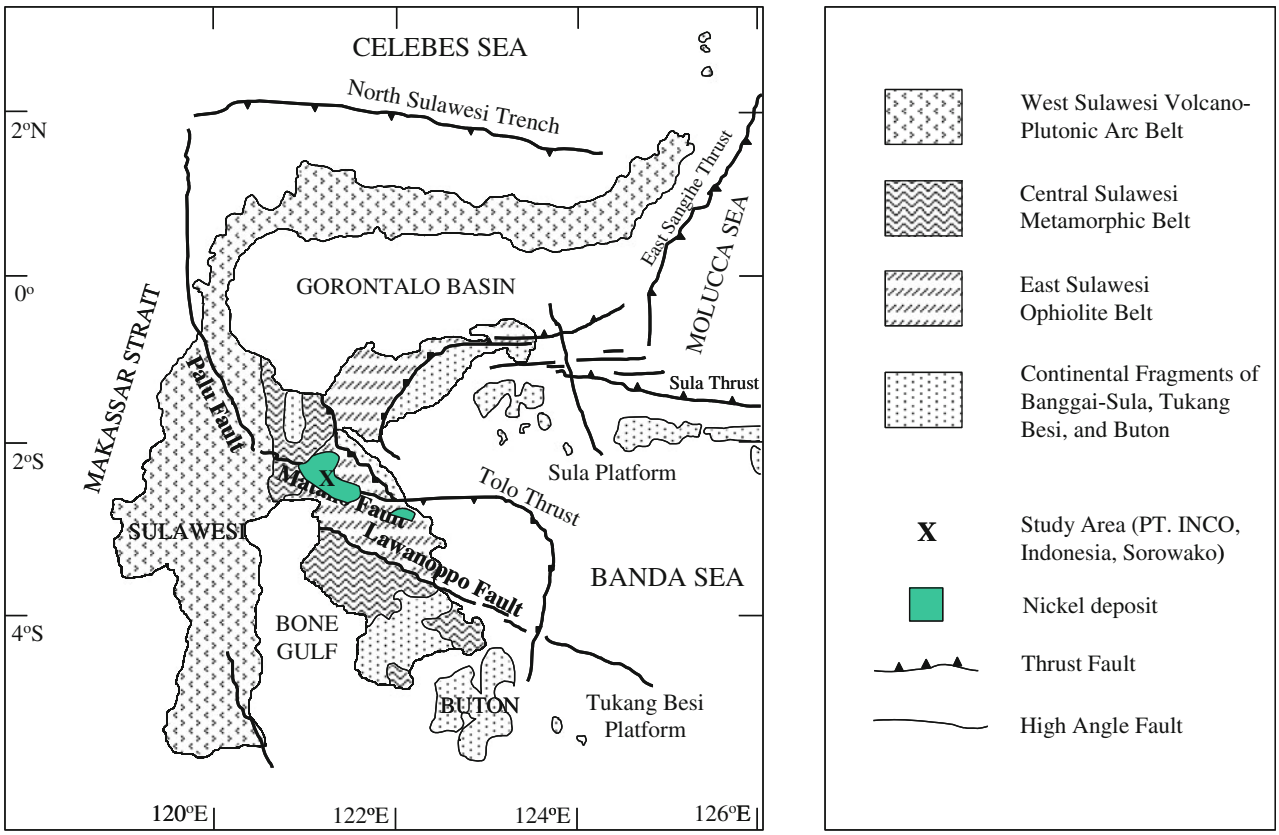

Figure 1. Location of study area (mining area of PT. INCO Indonesia) in South Sulawesi Province, Sulawesi Island, Indonesia with a geological map and four principal tectonic belts in Sulawesi Island (Mubroto et al. 1994).

strongly affect the rock-weathering rate, which determines the thickness of the laterization zone.

GEOLOGY AND DATA FOR ANALYSIS

Geological Setting

The generation of the laterite Ni deposits in the Sulawesi Island, Indonesia, is closely related to the setting of this island, which is at the convergence zone of three tectonic plates, Eurasian, Pacific, and Indian-Australian plates. Because of high tectonic activity, many active faults and extensional basins were developed throughout the Cenozoic era (Macpherson and Hall 2002), which made the geologic structures very complicated. This activity produced several huge ore deposits in a range of mineralization and metallogenic provinces.

Sulawesi Island consists of four principal tectonic belts (Fig. 1): the West Sulawesi Volcano-Plutonic Arc Belt, the Central Sulawesi Metamorphic Belt, the East Sulawesi Ophiolite Belt, and the Continental Fragments of Banggai-Sula, Tukang Besi, and Buton (Mubroto et al. 1994). The tectonic setting and physiography of Sulawesi Island were formed during the Neogene orogenesis that generated chains of mountains with peaks over 3,000 m a.s.l. and mineral deposits of laterite Ni, chromite, gold, and base metals in the East Sulawesi Ophiolite Belt. Laterite Ni deposits are mainly located in the complex of Cretaceous ultramafic rocks in the eastern Sulawesi and in the eastern coast zone (Fig. 1), which is composed of two Miocene rocks of subduction mélange of approximately 10 Ma (Golightly 1979; Suratman 2000). Most deposits are formed in hills and low mountains, which are deeply eroded and strongly weathered.

The geology of the Sorowako area and its surroundings can be divided mainly into three rock units: alluvial and sedimentary lacustrine rocks of Quaternary, Tertiary ultramafic rocks such as Harzburgite, and Cretaceous sedimentary rocks (Golightly 1979; Suratman 2000). Laterite Ni deposits in this area were generated in the Tertiary ultramafic rocks, which are a part of the serpentinized peridotite zone.

The study area is generally composed of unserpentinized ultramafic rocks. Laterite Ni deposits around the study area are classified as hydrous silicate deposits with harzburgite and dunite in the bedrocks (Gleeson et al. 2003). The weathered strata above the bedrock could be classified simply into two zones from the ground surface: the limonite and the saprolite zones, which were composed mainly of hematite and olivine, respectively. The average thicknesses of the limonite and saprolite zones are almost the same, 11 m (PT. INCO Indonesia 2006). Fine grain soils with red, brown, and yellow colors generally comprise the limonite zone. However, the saprolite zone is generally a mixture of soils with unweathered host rocks that retain their original texture and structure. Many fractures have developed in this zone due to weathering, with boulders forming between the fractures due to groundwater flowing through the fractures. Garnierite, which has a high Ni concentration, is usually found at the rim of these boulders. Below the saprolite zone, the bedrocks consist of unweathered ultramafic rocks whose upper parts are well fractured with garnierite and silicates present as filling minerals in the fractures.

Drillhole Data

Drillhole data at 294 sites were used for Ni grade modeling. The holes were drilled in a lattice pattern in a 1.6 km (E–W) by 1.0 km (N–S) area with a 50-m spacing between adjacent drillholes (Fig. 2). Drillholes were distributed along the ridges trending NE–SW. Because Ni-bearing minerals were concentrated in the weathered rocks, drillings were set to penetrate the weathered layer and reach the bedrock. The average depth of the 294 drillholes was 26.62 m.

The sample data collected at each site consisted of the concentrations (wt%) of four chemical components (Ni, Fe, SiO_2, and MgO), rock type, and the main constituent mineral. These data were measured from sub-cores of mostly 1-m length that were split from the original core sample. Accordingly, the data were collected at approximately 1-m depth intervals along the drillholes at each site. We initially examined the correlations between the Ni concentration and the other three components, but the correlations with Ni were all poor. Although the original sample data were multivariate, only the Ni data were used in the analyses because of this lack of correlation. Table 1 shows a part of the sample data at one site located on a hill.

GEOSTATISTICAL METHODS AND RESULTS

Selection of Influence Factor

The spatial variability of ore grade in a deposit is the most important feature for precise assessment

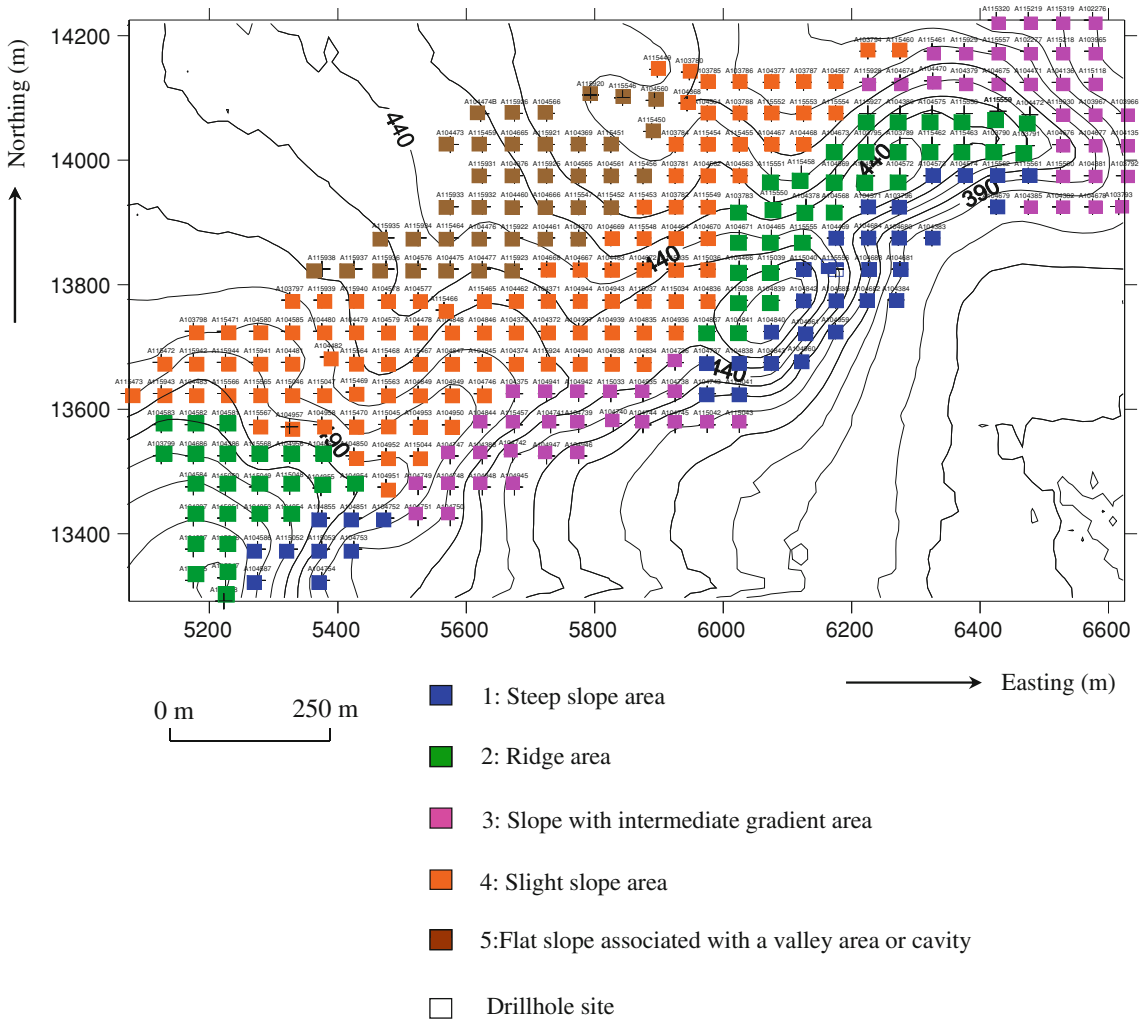

Figure 2. Drillhole distribution at 294 sites in the 1.6 km (E–W) and 1.0 km (N–S) area, superimposed upon the contour lines of topography. The sites were classified into the five categories of topographic features (see Fig. 3). Location in the study area is expressed using a plane rectangular local coordinate system in the mining area of PT. INCO Indonesia.

of ore reserves (Hartman 1992). Therefore, a proper spatial modeling technique, which interpolates and extrapolates the sample data of ore grade for unsampled points or blocks, is indispensable for this assessment. The success of geostatistics has been demonstrated in many case studies of ore grade estimation (e.g., Koike et al. 1998; Srivastava 2005; Verly 2005; Emery 2006). In addition, the identification of geologic factors that control the formation of the ore body and the heterogeneity of ore grade distribution is also significant (e.g., Koike and Matsuda 2006). Laterite Ni deposits, in general, are complicated in shape and chemical composition by several controlling factors related to climate, topographic condition, tectonic setting, lithofacies, parent rock type, geologic structure, groundwater, organic matter content, and rates of weathering (Brand et al. 1998; Gleeson et al. 2003). Depending on the size of each laterite deposit, the geomorphic factor may be the most predominant, because it can affect other factors such as the groundwater system, weathering processes, and geological features, on the layer thickness of the laterization zone (limonite and saprolite zones) above bedrock.

Thus, the geomorphic factor was expressed in this study of Ni grade modeling by classifying the topography into five categories. These are: (1) steep slope (gradient ≥45°); (2) ridge (regions near the line of a ridge with gradient <45°); (3) slope with intermediate gradient (gradient ≥20°); (4) slight slope (gradient ≥5°); and (5) flat slope with a gradient <5°, which is associated with a valley area, or cavity

Table 1. Example of Drillhole Sample Data Composed of Four Chemical Concentrations, Rock Type, and Main Constituent Mineral

Drillhole Number	Depth Range (m)	Ni (wt%)	Fe (wt%)	SiO_2 (wt%)	MgO (wt%)	Layer	Rock Type	Primary Mineral
A104378	0.20–1.00	1.16	47.20	7.00	1.20	lim		hmt
A104378	1.00–2.00	0.33	6.60	36.00	42.50	lim		hmt
A104378	2.00–3.00	1.21	43.40	9.00	1.30	lim		hmt
A104378	3.00–4.00	1.53	44.50	7.70	1.50	lim		hmt
A104378	4.00–5.00	1.32	44.40	7.10	1.40	lim		hmt
A104378	5.00–6.00	1.32	43.60	7.80	1.40	lim		hmt
A104378	6.00–7.00	1.32	34.80	24.50	5.00	lim		hmt
A104378	7.00–8.00	1.46	44.10	9.90	1.50	lim		hmt
A104378	8.00–9.00	1.21	28.20	26.80	5.10	sap		hmt
A104378	9.00–10.00	1.81	9.58	39.54	27.19	sap	hrz	olv
A104378	10.00–10.55	2.03	10.65	39.30	26.22	sap	hrz	olv
A104378	10.55–11.00	0.52	8.30	41.20	48.50	sap	hrz	olv
A104378	11.00–12.00	0.20	7.00	73.20	0.30	sap	hrz	olv
A104378	12.00–12.40	2.13	11.40	40.60	28.70	sap	hrz	olv
A104378	12.40–13.00	0.26	6.40	39.00	48.50	sap	hrz	olv
A104378	13.00–13.55	1.59	10.70	31.90	24.70	sap	hrz	olv

The depth ranges of data at all sites were classified into three layers, limonite, saprolite, and bedrock.
lim limonite, *sap* saprolite, *hrz* harzburgite, *hmt* hematite, *olv* olivine.

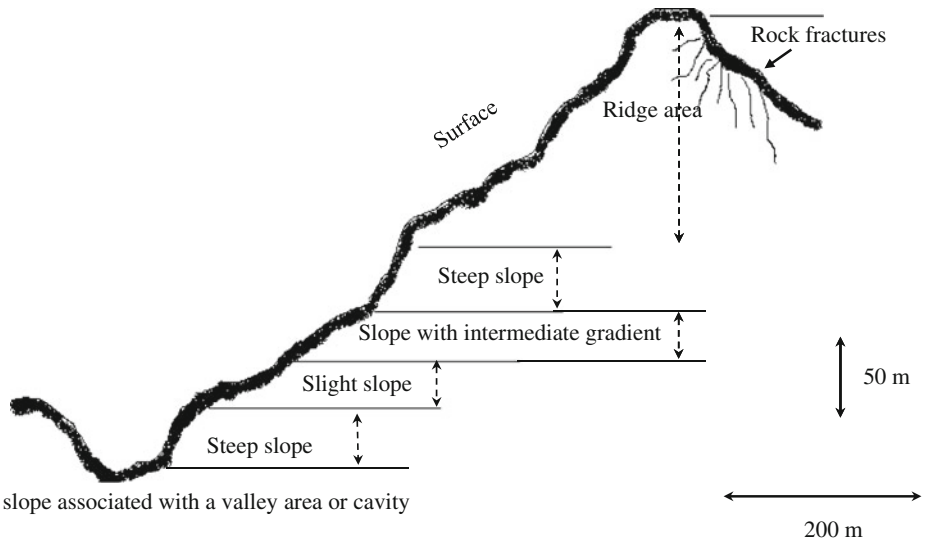

Figure 3. Schematic map of topographic features classified into five categories by slope gradient (steep slope, ridge, slope with intermediate gradient, slight slope, and flat slope associated with valley area or cavity).

feature (Fig. 3). These five categories are consistent the first proposal that considered topography for Ni grade characterization (Darijanto 1999) which suggested that the thickness of the laterization zones and the resultant Ni grades were correlated with these geomorphic features, and the terrain classification based on the slope angle by Van Zuidam (1985). Suitable threshold angles for the categories were defined in this study by considering the local minimums from the histograms of slope angles. Slope gradient can control the infiltration rate of surface water into the ground, which further affects weathering of rocks and the enrichment processes of Ni. In addition, slope gradient can characterize geomorphology simply when the study area is small. Based on this criterion, the drillhole sites were classified into: steep slope (37 sites), ridge (56 sites), slope with intermediate gradient (57 sites), slight slope (105 sites), and flat slope (39 sites), as shown in Figure 2. This figure shows that the steep slope and

ridge areas are situated on the northeast and the southwest sides; intermediate gradient areas are near the northeastern and the southern edges; and the slight slope and flat areas are in the central and northern parts of the study area.

Correlation Analysis

In general, there is a relationship between slope gradient and thickness of the laterization zone, which was caused by differences in weathering processes depending on geomorphology (Ahmad 2001). To confirm this general relationship, the average thickness of the limonite zones was calculated at every category of topographic feature as shown in Figure 4. Clearly, the average thickness tends to increase with a decrease in slope gradient. This trend was further examined by considering the topographic detail under the following two specific conditions. Because the lithologies and rock properties in a laterite Ni deposit are known to be highly heterogeneous (e.g., Gleeson et al. 2003), we examined the trend more precisely using only neighboring data.

The first condition was to select the drillholes located close to each other at the same elevation in the same category (Fig. 5a). Such data were considered to be in the same geological environment. For category 1, only three drillholes were at the same elevation (390 m) and were used for calculating the average thickness of the limonite and saprolite zones. Their averages were 3.72 and 12.02 m, respectively

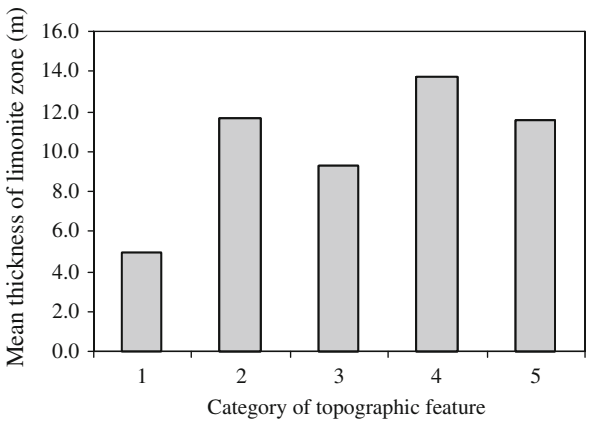

Figure 4. Correlation between the category of topographic features (first to fifth category depending on slope gradient as defined in Fig. 2) and mean thickness of the limonite zones in each category. Slope gradient decreases from first to fifth category.

(Table 2). For category 2, four drillholes located on 410 m were selected as shown in the table. The second condition for selecting the drillholes was that they should be located close to a straight line that was in the direction of maximum gradient (Fig. 5b). This selection was intended to use the data that were considered to be under the same weathering process. For category 1, four drillholes satisfying this condition were at elevations of 460, 440, 410, and 380 m and the results are shown in Table 2.

Results from Table 2 of the mean thicknesses of the limonite zones in the five categories are depicted in Figure 6. Both sets of results for these topographic conditions show the characteristic that the thickness increased with a decrease in slope gradient is more precise than for the gross analysis in Figure 4. In general, limonite forms the top layer in laterite deposit areas. Therefore, slope gradient is identified as an important factor for controlling weathering depth of the limonite zone; flat topography causes a thicker weathering zone in the shallow depth range, because of greater infiltration of rain and surface water.

But, the thickness of the saprolite zone below the limonite zone has no correlation with the thickness of the limonite zone as shown in Figure 7a (coefficient of determination $R^2 = 0.01$). This poor correlation is the same for the data at the same elevation selected by the first condition ($R^2 = 0.03$) (Fig. 7b). Therefore, mechanism and dominant factors of weathering on the formation of the saprolite zones were different from the limonite zone. Plausible dominant factors on the formation of the saprolite zone are geological structure, drainage pattern, and the position of the water table. These factors coupled with the maximum rates of leaching and drainage of the subsequent solution enhanced both the residual concentration and the accumulation of Ni in the saprolite zone (Gleeson et al. 2003).

Changes in Ni grade with depth at each drillhole site were characterized for every category of topographic feature. Figure 8a, b, c, and d are the data on slight slope, flat slope, ridge, and steep slope areas, respectively. The limonite zones are relatively thick on the gently sloping areas (a and b), but thin at the steep areas (c and d). Common to the four graphs, the Ni grade increases from the limonite to saprolite zones and reaches a maximum (enclosed by circle) in the saprolite zones. The grades are low in the bedrock zone. Figure 8 highlights the fact that the Ni grades change abruptly within the saprolite zone and their average values are similar among the

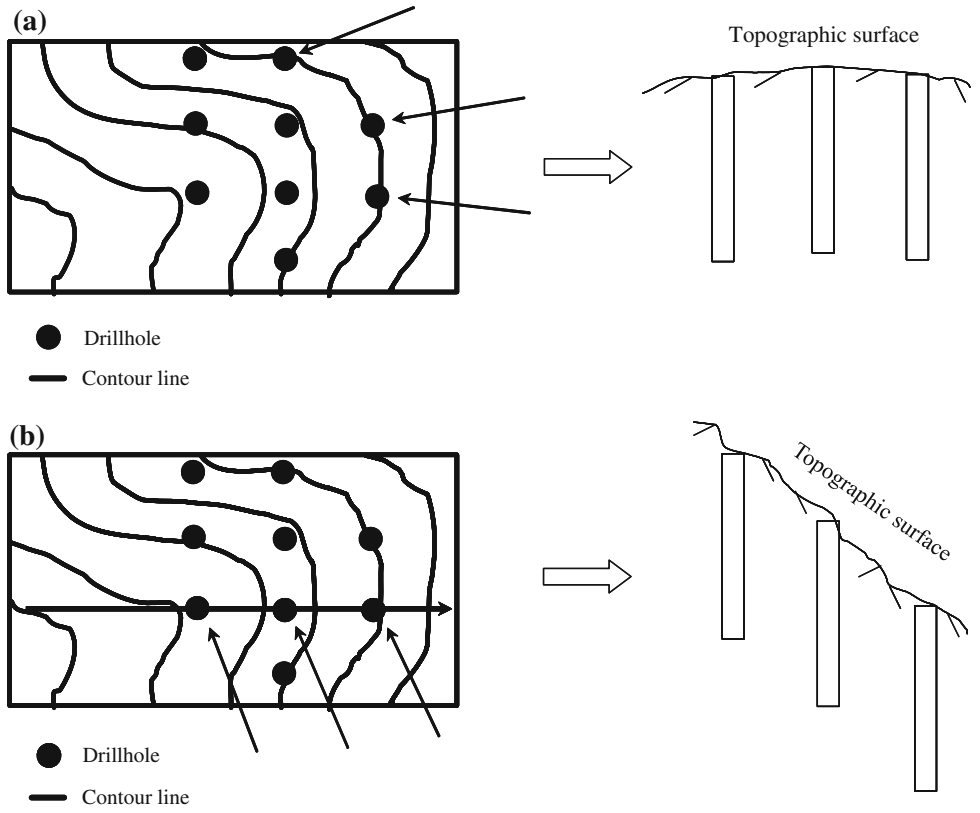

Figure 5. Two conditions for selecting the drillholes in the same category to identify relationships between the slope gradient and the thickness of laterization zone, in particular limonite zone in detail, which are for drillholes located (a) on the same elevation and (b) along a straight line in the direction of the maximum gradient.

Table 2. Mean Thicknesses of Limonite and Saprolite Zones and the Maximum Ni Grade in the Saprolite Zone at Each Category of Topographic Feature

			Value		
			Mean Thickness (m)		
Drillhole Location	Category of Topographic Feature	Number of Drillholes	Limonite Zone	Saprolite Zone	Mean of Maximum Ni Grade in the Saprolite Zone (wt%)
Same elevation	1	3	3.72	12.02	1.88
	2	4	8.33	11.45	1.88
	3	3	11.85	2.03	1.56
	4	7	14.80	13.80	3.55
	5	4	13.30	9.75	2.11
Different elevations	1	4	2.75	11.76	2.19
	2	5	7.06	11.03	2.52
	3	5	9.49	5.86	2.00
	4	7	17.25	13.16	3.03
	5	6	13.06	11.87	2.95

Sample data were classified into two groups: the sites located at similar elevations and the other sites at different elevations by the two methods in Figure 5.

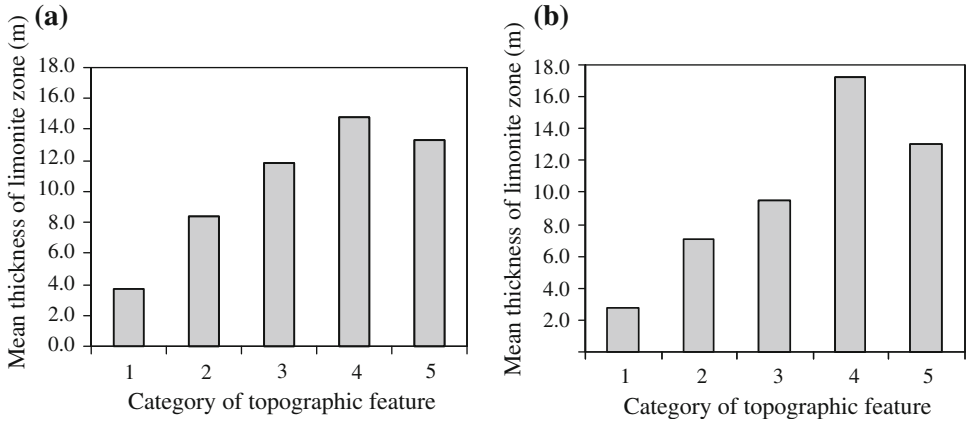

Figure 6. Relationships between the categories of topographic feature and the average thicknesses of the limonite zone using drillhole data located (a) on the same elevation and (b) along the maximum gradient of slope selected by the two conditions in Figure 5.

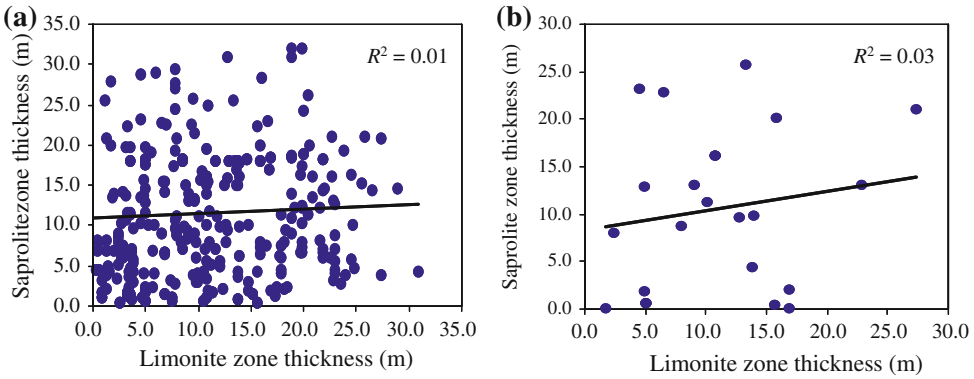

Figure 7. Scattergrams between the thicknesses of limonite and saprolite zones using (a) all drillhole data and (b) drillhole data at the same elevations selected by the method in Figure 5a.

four categories. As an example, the averages of Ni grade data are similar over all drillhole sites and therefore, the use of averages leads to ambiguous correlations between geomorphology and Ni grade, and to featureless mapping of Ni grade in the saprolite zone. The maximum Ni grade is variably attributable to the degree of weathering, lithofacies, and topographic features such as the slope gradient. Moreover, the maximum Ni grade in the saprolite zone is significant for identifying the most promising location of the Ni resource and developing a mine plan and design. Therefore, the saprolite zone is a target for Ni mining and the maximum Ni grade in this zone can be an indicator for predicting the lifetime of a mine. This is a compelling reason for using the maximum Ni grade for spatial modeling.

It is noted that the thickness of the saprolite zone was generally well correlated with the maximum Ni grade in this zone as shown in Figure 9. Although the data were scattered around the regression lines, the maximum Ni grade tends to increase with increasing layer thickness and this trend is common to all five categories (the maximum R^2 for category 2 was $R^2 = 0.23$; and the minimum for category 3 was $R^2 = 0.11$) and to the overall data ($R^2 = 0.26$). The saprolite zone is known to become thick in a well-fractured area, because the groundwater easily infiltrates through rock fractures, causing deep weathering. Ni grade tends to be high in this circumstance, due to high levels of leaching and chemical reaction within fractured rocks, in particular under tectonic uplift (Gleeson et al. 2003).

CO-KRIGING FOR NI GRADE MODELING

Co-kriging is a method for estimation that minimizes the variance of the estimation error by

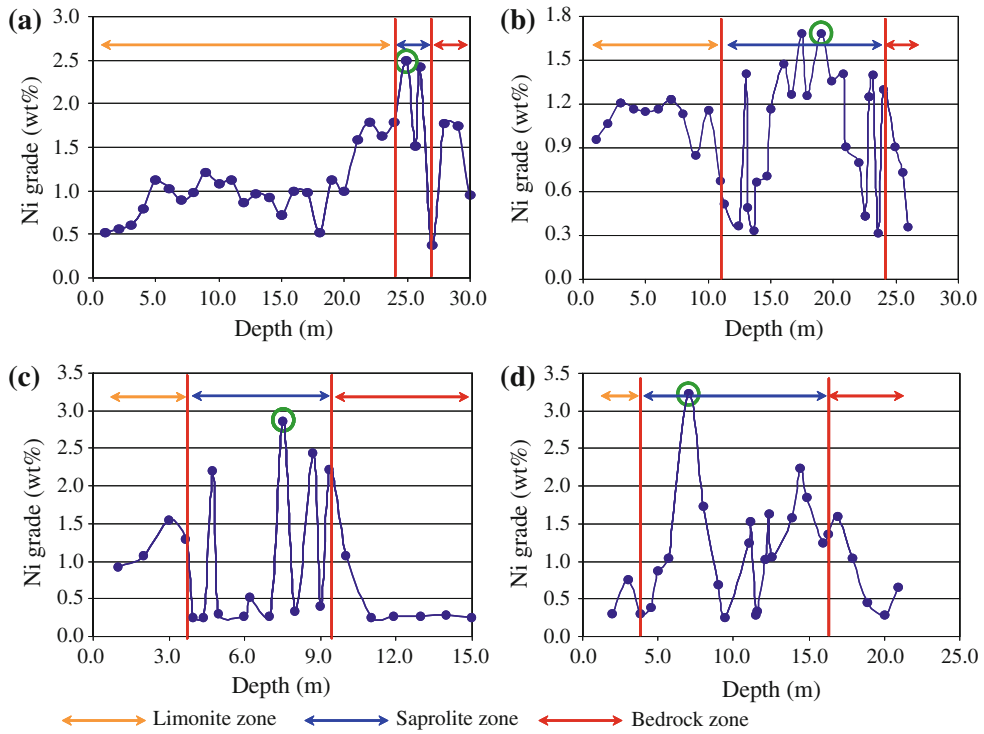

Figure 8. Changes in the Ni grades with depth at four drillhole sites at (a) slight slope, (b) flat slope, (c) ridge, and (d) steep slope areas. Open circle denotes the maximum Ni grade at each drillhole.

exploiting the cross-correlation between several variables; the estimates are derived using supplementary variables, as well as the primary variable (Isaaks and Srivastava 1989). Co-kriging techniques have been applied widely to metal and nonmetal resource analyses on maps of ore grade, resource quality, and reserve assessment (e.g., Dowd 1992; Koike and Matsuda 2006; Heriawan and Koike 2008; Juan et al. 2011). In the case of two variables only, the ordinary co-kriging estimate is a linear combination of the values of the primary and secondary variables as:

$$\hat{w} = \sum_{j=1}^{n} b_j \cdot w_j + \sum_{i=1}^{m} a_i \cdot v_i$$
$$\sum_{j=1}^{n} b_j = 1, \quad \sum_{i=1}^{m} a_i = 0 \tag{1}$$

where w_j and v_i are the primary and secondary variables at n and m nearby locations around the location to be estimated, respectively, $\hat{w}$ is the estimated value, and a_i and b_j are the co-kriging weights that can be obtained from the semivariogram and cross-semivariogram of the two variables. For standardized ordinary co-kriging, the nonbiased condition is changed to:

$$\sum_{j=1}^{n} b_j + \sum_{i=1}^{m} a_i = 1 \tag{2}$$

Because of the general correlation between the maximum Ni grade in the saprolite zone, which was defined as the primary variable, and the thickness of the saprolite zone as the secondary variable, co-kriging was adopted for spatial modeling of the primary variable. ArcGIS® Geostatistical Analyst (ver. 10) was used for the following variography and kriging calculations. Experimental semivariograms of each variable and a cross-semivariogram of the two variables, $\gamma(h)$s, were calculated in the horizontal direction using 50 m as the unit of lag distance. As described above, the depths of the drillholes were much shallower than the size of study area, and suitable $\gamma(h)$ values could not be obtained in the vertical direction. Thus, we only considered the horizontal direction for the variography. The resultant omnidirectional $\gamma(h)$s could be fitted by spherical models as shown in Figure 10. The nugget effect on the $\gamma(h)$ of the maximum Ni grade in the

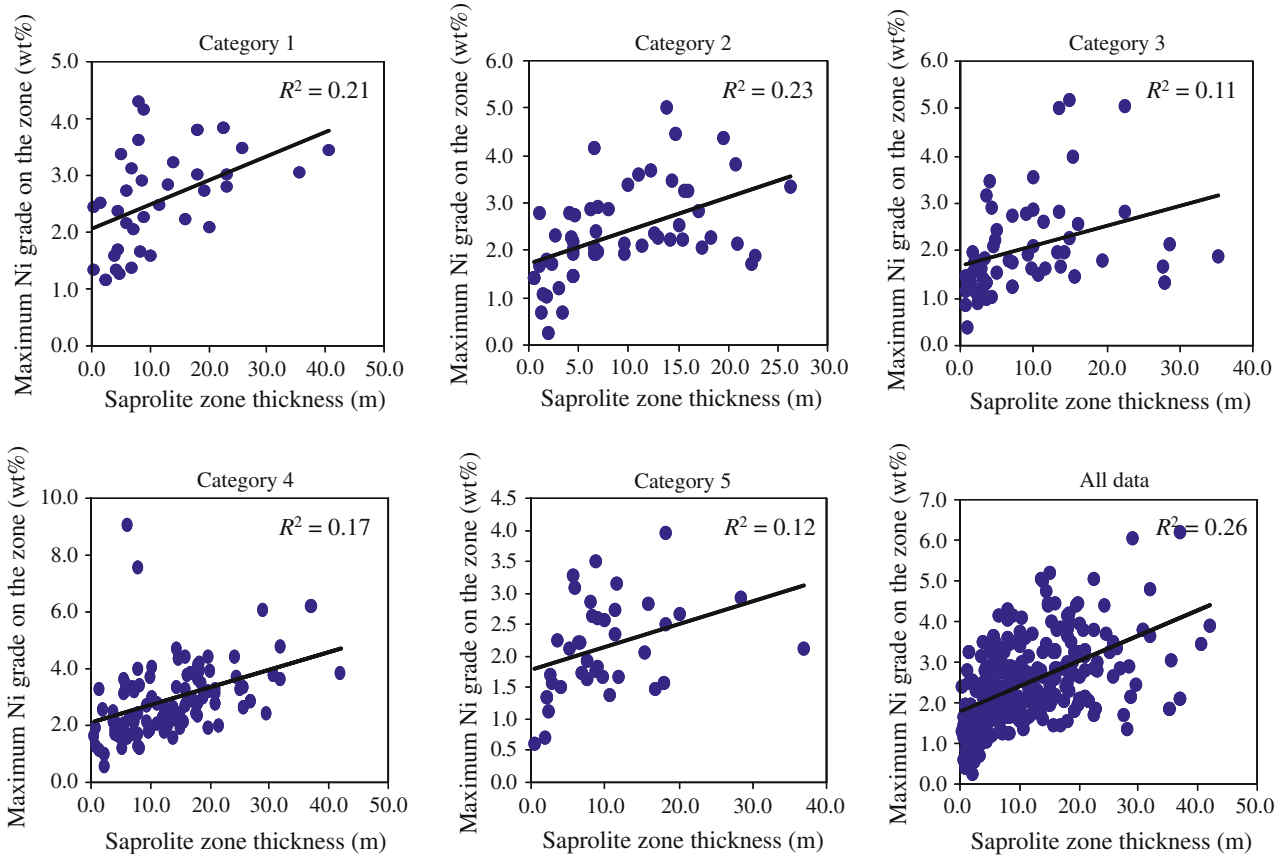

Figure 9. Scattergrams between the saprolite zone thickness and the maximum Ni grade of the zone for every category of topographic feature and for all drillhole data. See Figure 2 for the detail of the category.

saprolite zone is the largest and the ranges of $\gamma(h)$ for each variable (110 and 90 m) are less than the range of $\gamma(h)$ of the two variables combined (145 m). This result demonstrates the effectiveness of combining the maximum Ni grade in the saprolite zone with the thickness of the saprolite zone for the spatial modeling of Ni grade.

Co-kriging calculations on the distribution of the maximum Ni grade in the saprolite zone were implemented using a grid spacing of 10 m. The following discussion is based on the standardized ordinary co-kriging result, which gave a better estimation than ordinary co-kriging. The estimated distribution highlights clear anisotropy along NE–SW corresponding with the topography. The result overlaid topographic features (Fig. 11a), and a perspective view of the topography (Fig. 11b) clarifies the finding that the maximum Ni grade tended to be high mainly at the slight slope area, which may be attributable to the enrichment processes of Ni at these topographic features. Deep and strong weathering caused by rock fractures may have occurred in such groundwater-rich zones and accordingly, the thick laterization zones that were formed were conducive to the accumulation of Ni. Enlargement of the highest grade zone in Figure 11a reveals large variability in the grades on a much smaller scale than the interval of two adjacent drillhole sites (50 m). High and low grades were estimated locally at sample sites. This characteristic proves the preciseness of the co-kriging.

Figure 12 represents a cross-validation between the measured and the predicted co-kriging values of the maximum Ni grade. The coefficient of correlation between the two values (R) is 0.83 and the root mean square (RMS) error is 0.80. The co-kriging result was compared with the ordinary kriging result using a single variable (i.e., the maximum Ni grade in the saprolite zone). The maximum Ni grade distribution determined by ordinary kriging, as shown in Figure 13a, is much smoother than the co-kriging model and featureless. This smoothing effect

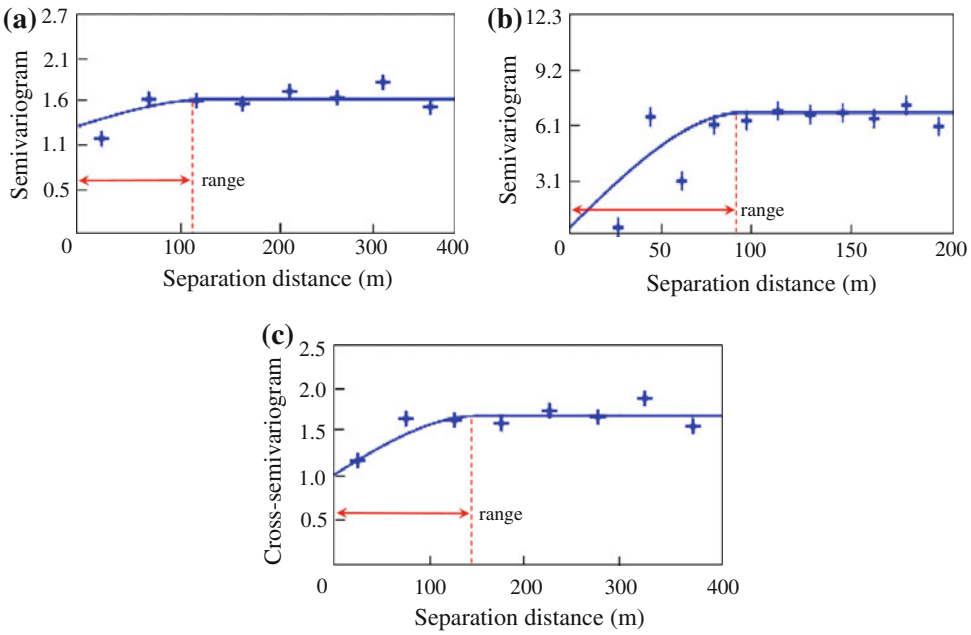

Figure 10. Omnidirectional semivariograms of: (a) the maximum Ni grade in the saprolite zone; (b) the thickness of zone; and (c) a cross-semivariogram combining these two variables. Spherical models were used to fit all the semivariograms. Each dot represents the semivariances at each separation distance.

appeared clearly in the cross-validation graph in Figure 13b, where the regression line is much gentler than for the co-kriging (Fig. 12) or the 45° line. The RMS error for ordinary kriging is 1.11, which is larger than the co-kriging RMS value. The superiority of co-kriging over ordinary kriging is clearly shown by these comparisons, and consequently, the co-kriging result can be regarded as providing sufficient accuracy.

To examine the relationships between the topographic features and the formation of the saprolite zone, and the maximum Ni grade distribution, the mean and upper and lower quartile values of the thickness of the saprolite zones and the maximum Ni grades on the saprolite zones at the five topographic features were calculated, as shown in Figure 13. This figure clarifies that the thick saprolite zone and the maximum Ni grade are located generally at the slight slope area. Consequently, topography is confirmed to be a strong factor determining Ni grade distribution.

DISCUSSION

In laterite Ni deposits, many rock fractures tend to be developed at slight slopes, steep slopes, and ridge areas, because the rocks in such areas are relatively hard with considerable resistance to erosion. As demonstrated in Figure 14, the saprolite zone is thick in the slight slope, steep slope, and ridge areas. Therefore, the thick saprolite zone may have formed by the existence of many rock fractures that have functioned as a path for groundwater because of high hydraulic conductivity. It is known that the infiltration of groundwater through the fractures causes rapid leaching of Ni in the upper saprolite zone and also rapid deposition of Ni in the lower saprolite zone (Ahmad 2001). In fact, rock fractures are developed at every topographic feature in the study area, but the slight slope is the most fractured, due to the reverse fault movements under the regional tectonic stress field. Figure 15 shows examples of rock fractures at slight slope, steep slope, and ridge areas, which confirm a dense distribution of fractures almost all filled with garnierite.

High Ni grade at the slight slope area depicted in Figure 11 confirms that this topographic feature is a catchment capable of gathering much rain and surface water, which in part becomes groundwater. Groundwater causes leaching and enrichment of Ni, as well as causing the fractured zones and deep weathering of both the limonite and the saprolite zones. As a result, both zones become thicker with a high Ni grade peaking on the slightly sloping areas.

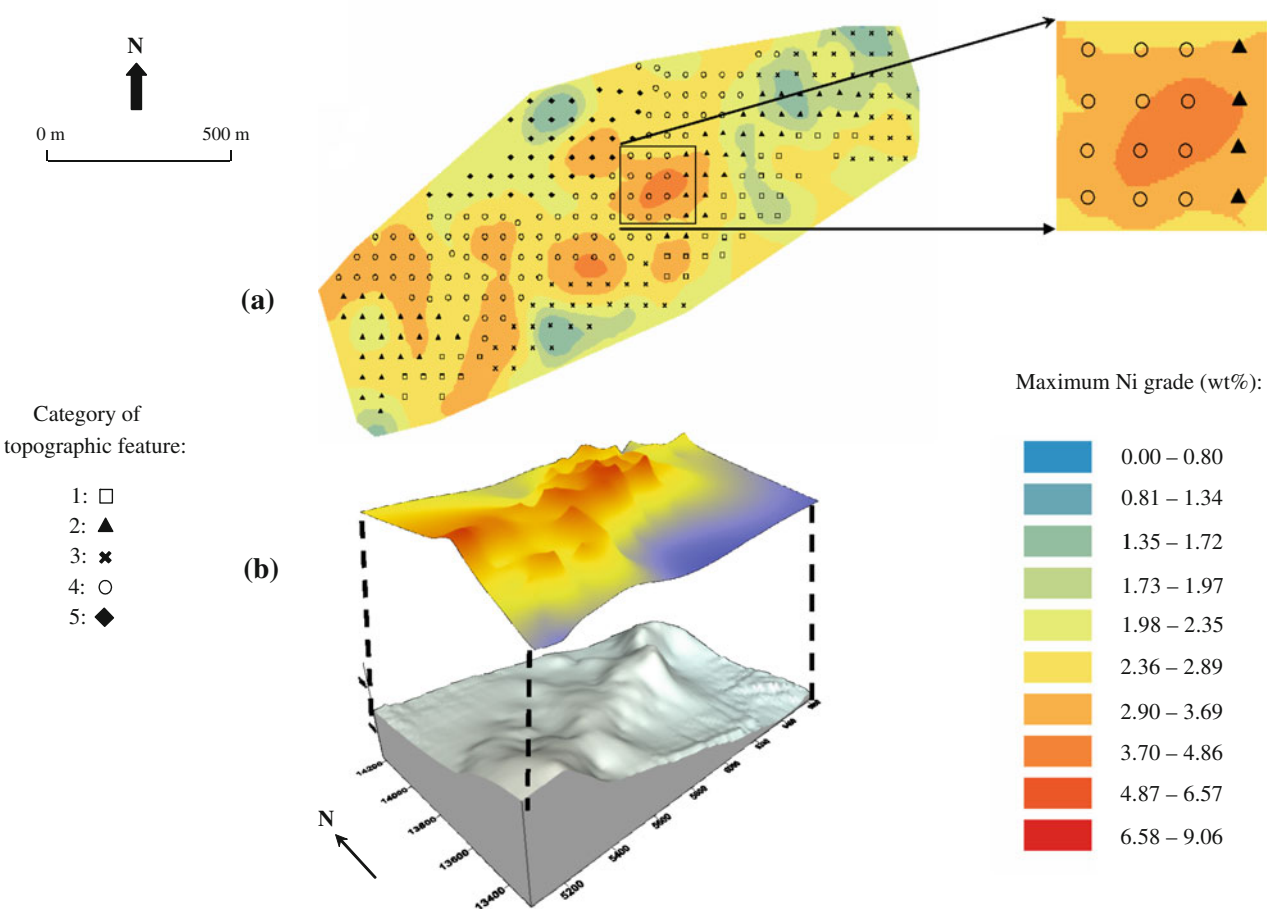

Figure 11. Distribution of the maximum Ni grade in the saprolite zone by co-kriging superimposed upon (a) the category of topographic feature and (b) a perspective view of topography. Enlargement of the highest grade zone is included in (a).

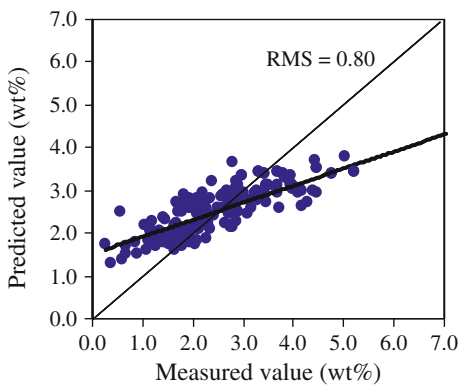

Figure 12. Scattergram for cross-validation of co-kriging accuracy between measured and predicted co-kriging values of the maximum Ni grade in the saprolite zone.

CONCLUSION

For precise spatial modeling of Ni grade in a laterite deposit, this study identified factors controlling the grade distribution and then applied geostatistical techniques to a world-famous Ni deposit area in Sulawesi Island, Indonesia. At first, geomorphic characteristics such as topographic features and the thickness of the laterization zone (limonite and saprolite zones above the bedrock) and the maximum Ni grade in the saprolite zone were used for the correlation analysis between every pair of sites in the dataset. The topographic features were classified into five categories depending on the magnitude of slope gradient from steep to flat areas. The slope gradient was shown to have a strong spatial correlation with the

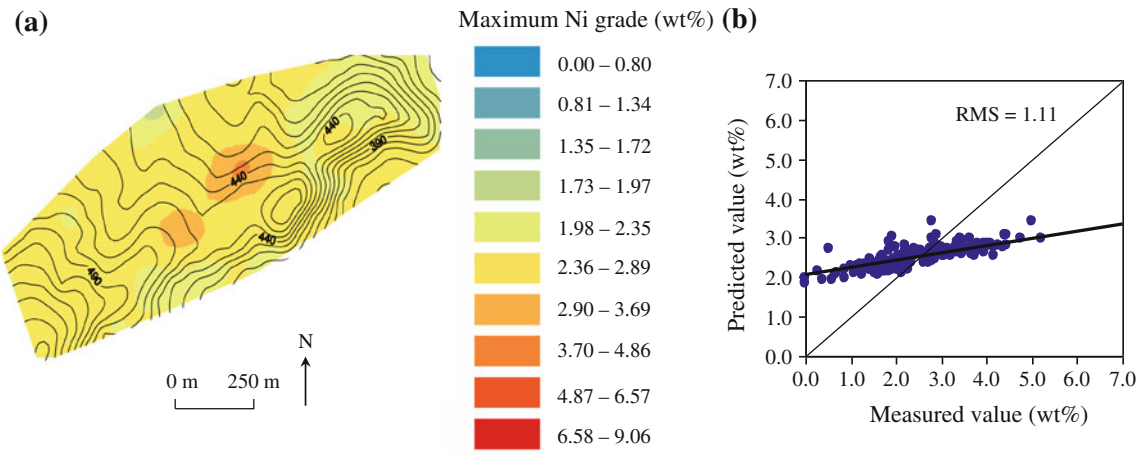

Figure 13. Distribution of the maximum Ni grade in the saprolite zone by ordinary kriging analysis (a) and a scattergram showing the cross-validation of the ordinary kriging accuracy (b).

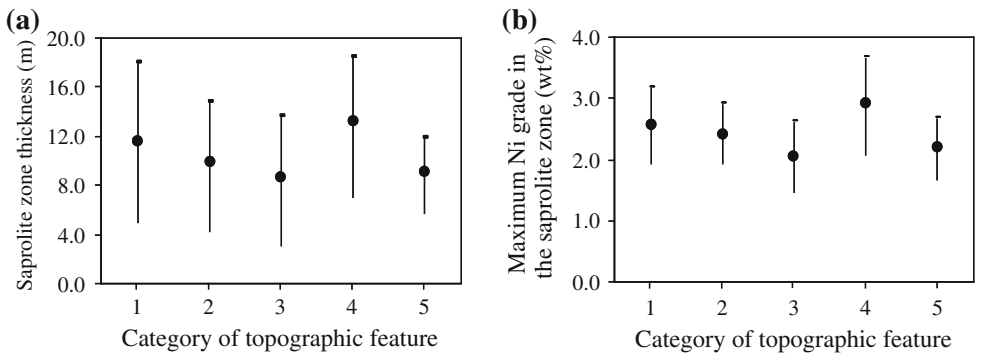

Figure 14. Relations of the mean (closed circle) and the upper and lower quartiles (top and bottom of bar) of (a) the thickness of saprolite zone and (b) the maximum Ni grade in the zone to category of topographic feature.

thickness of the limonite zone; the thickness of the limonite zone increased with a decrease of the slope gradient. On the other hand, there were no correlations in the thickness between the saprolite and the limonite zones, and between the slope gradient and the thickness of saprolite zone. The most important trend was a general spatial correlation between the thickness of the saprolite zone and the maximum Ni grade in that zone; the maximum Ni grade in the saprolite zone increased with the thickness of the zone.

Because the maximum Ni grade in the saprolite zone is one of the foremost properties for mine planning and description of a laterite Ni deposit, co-kriging was adopted to construct a distribution model of the grade with respect to the correlation with the thickness of the saprolite zone. The resultant co-kriging model highlighted that the maximum Ni grades in the saprolite zone were generally highest at the slight slope area. Ni accumulation at this area probably originates from deep weathering caused by the development of rock fractures and passing of groundwater through the fractures from significant water catchments.

ACKNOWLEDGMENTS

The authors express their sincere thanks to PT. INCO Indonesia for permission to use the data set. Sincere thanks must be extended to Absar, Sudarmin, Malik Hakim Sopi, Ade Kadarusman, Robby Rafianto, Mashury, Amir Mahmud, Arifin, Kamto, Yonas, Aliahni Djafar, Selvi Yuminti, and Asriani for their constructive help in the field and in the office, and furthermore to anonymous two reviewers

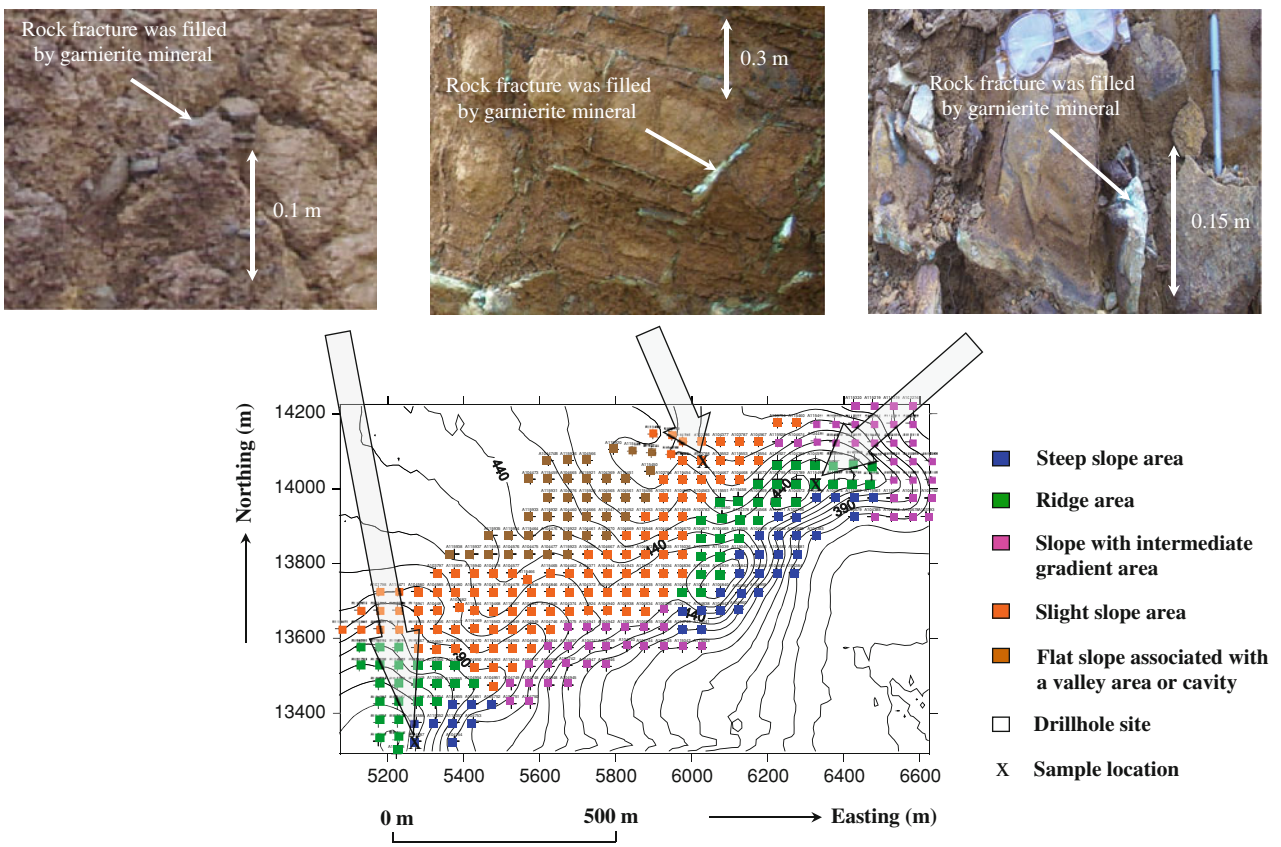

Figure 15. Examples of rock fractures in the saprolite zone at ridge area (right), slight slope area (middle), and steep slope area (left). Almost all fractures are filled with garnierite.

for the valuable comments and the detailed suggestions that helped improve the clarity of the manuscript.

REFERENCES

Ahmad, W. (2001). *Chemistry, mineralogy and formation of Ni laterites* (pp. 41–54). Sorowako: PT. INCO Indonesia.

Brand, N. W., Butt, C. R. M., & Elias, M. (1998). Nickel laterites: Classification and features. *Australian Geology and Geophysics, 17*(4), 83–88.

Darijanto, T. (1999). The influence of morphology to the formation and distribution of laterite nickel deposits. In *Proceedings of 8th Indonesian association of mining experts* (pp. 1–18). Bandung, Indonesia.

Dowd, P. A. (1992). Geostatistical ore reserves estimation: A case study in a disseminated nickel deposit. *Geological Society of London Special Publications, 63*, 243–255.

Emery, X. (2006). Two ordinary kriging approaches to predicting block grade distributions. *Mathematical Geology, 38*(7), 801–819.

Gleeson, S. A., Butt, C. R. M., & Elias, M. (2003). Nickel laterites: A review. *Society of Economic Geologists Newsletter, 54*, 9–16.

Golightly, J. P. (1979). *Geology of Soroako nickeliferous laterite deposit*. Ontario, Canada: INCO Metals Company.

Hartman, H. L. (1992). *Mining engineering handbook* (Vol. 1, pp. 344–347). Denver, CO: Society for Mining, Metallurgy and Exploration, Inc.

Heriawan, M. N., & Koike, K. (2008). Uncertainty assessment of coal tonnage by spatial modeling of seam distribution and coal quality. *International Journal of Coal Geology, 76*, 217–226.

Isaaks, E. H., & Srivastava, R. M. (1989). *An introduction to applied geostatistics* (pp. 400–416). Oxford: Oxford University Press, Inc.

Juan, P., Mateu, J., Jordan, M. M., Mataix-Solera, J., Malendez-Pastor, I., & Navarro-Pedreno, J. (2011). Geostatistical methods to identify and map spatial variations of soil salinity. *Geochemical Exploration, 108*(1), 62–72.

Koike, K., Gu, B., & Ohmi, M. (1998). Three-dimensional distribution analysis of phosphorus content of limestone through a combination of geostatistics and artificial neural network. *Nonrenewable Resources, 7*(3), 197–210.

Koike, K., & Matsuda, S. (2006). New indices for characterizing spatial models of ore deposits by the use of a sensitivity vector and an influence factor. *Mathematical Geology, 38*(5), 541–564.

Macpherson, C. G., & Hall, R. (2002). Timing and tectonic controls in the evolving orogen of SE Asia and the western Pacific and some implications for ore generation. *Geological Society of London Special Publications, XXX*, 1–19.

Mubroto, B., Briden, J. C., McClelland, E., & Hall, R. (1994). Paleomagnetism of the Balantak ophiolite, Sulawesi. *Earth and Planetary Science Letters, 125*, 193–209.

Price, J. G. (2010). The world is changing, View I. *Society of Economic Geologists Newsletter, 82*, 12–14.

PT. INCO Indonesia. (2006). Inventory of mineral resources and mineral reserves, Unpublished report (in Bahasa Indonesia).

Srivastava, R. M. (2005). Probabilistic modeling of ore lens geometry: An alternative to deterministic wireframes. *Mathematical Geology, 37*(5), 513–544.

Sufriadin, Idrus, A., Pramumijoyo, S., Warmada, I. W., Yonezu, K., & Imai, A. (2010). Characterization and leaching behavior of minerals by sulphuric acid in the Sorowako nickeliferous ores, Sulawesi, Indonesia. In *Proceedings of international symposium on earth science and technology, Fukuoka, Japan* (pp. 421–425).

Suratman. (2000). Geology of laterite nickel deposit in Sorowako area, South Sulawesi Province. In *Proceedings of 29th Indonesian association of geologists, Bandung, Indonesia* (pp. 37–43).

Thompson, S. A. (2000). An overview of nickel-titanium alloys used in dentistry. *International Endodontic Journal, 33*, 297–310.

Thorne, R., Herrington, R., & Roberts, S. (2009). Composition and origin of the Caldag oxide nickel laterite, W. Turkey. *Mineralium Deposita, 44*, 581–595.

USGS. (2011). *Nickel: Mineral commodity summaries* (pp. 108–109). Reston, VA: U.S. Geological Survey.

Van Zuidam, R. A. (1985). Terrain analysis and classification using aerial photographs. In *ITC-Textbook* (2nd ed., VII-6). International Institute for Aerial Survey and Earth Sciences, Enschede, Netherland.

Verly, G. (2005). Grade control classification of ore and waste, a critical review of estimation and simulation based procedures. *Mathematical Geology, 37*(5), 451–475.